Published in final edited form as:
Sci Transl Med. 2009 October 14; 1(2): 2ra6. doi:10.1126/scitranslmed.3000289.

Arrhythmia in Heart and Brain: KCNQ1 Mutations Link Epilepsy and Sudden Unexplained Death

A. M. Goldman, **E. Glasscock**, **J. Yoo**, **T. T. Chen**, **T. L. Klassen**, and **J. L. Noebels**
Department of Neurology, Baylor College of Medicine, Houston, TX 77030

Abstract

Sudden unexplained death in epilepsy (SUDEP) is a catastrophic complication of human idiopathic epilepsy, with an estimated prevalence of up to 18%. A molecular mechanism and an identified therapy have remained elusive. Here we find that epilepsy occurs in mouse lines bearing dominant human LQT1 mutations for the most common form of cardiac long QT syndrome (LQTS), which causes syncopy and sudden death. *KCNQ1* encodes the cardiac KCNQ1 (KvLQT1) delayed rectifier channel, which has not been previously localized to the brain. We have shown that it is expressed in forebrain neuronal networks and brainstem nuclei, regions in which a defect in the ability of neurons to repolarize after an action potential can produce seizures and dysregulate autonomic control of the heart. That LQTS mutations in this gene cause epilepsy reveals the dual arrhythmogenic potential of an ion channelopathy co-expressed in heart and brain, and motivates a search for genetic diagnostic strategies to improve risk prediction and prevention of early mortality in persons with seizure disorders of unknown origin.

INTRODUCTION

Sudden unexplained death in epilepsy (SUDEP) accounts for 2% – 18% of mortality in epilepsy, which exceeds the expected rate in the general population by nearly 24 times (1,2). By definition, postmortem examination does not reveal the cause of death or evidence of primary pulmonary or cardiac pathology. The commonly cited clinical risk factors predisposing to SUDEP are: early onset intractable epilepsy, male sex, age 20 to 40 years, generalized seizures, exposure to multiple anticonvulsant medications, and poor compliance with medications (3). Apnea due to central respiratory depression and cardiac failure mediated by autonomic dysregulation are two major pathogenic mechanisms implicated in SUDEP (4). Since Russell first documented cardiac asystole during a seizure in 1906, a wide range of cardiac arrhythmias thought to be of cerebral origin have been reported, ranging from atrial fibrillation, supraventricular tachycardia, prolonged QT intervals, and torsades de pointes (4, 5), supporting the idea that “arrhythmogenic epilepsy” is one of many possible SUDEP mechanisms. Although neural defects leading to cardiorespiratory arrest have long been suspected, the biological mechanisms of SUDEP have never been confirmed and their direct link to cortical hyperexcitability has not been identified.

Among many potential cardiac pathologies for SUDEP, focus has recently shifted to a specific set of molecular targets, the LQT genes. The long QT syndrome (LQTS) is a well recognized cause of fatal ventricular arrhythmias and sudden unexplained death in young people and can be caused by mutations in 10 or more genes, including 8 ion channels (6). Mutations in these

Author contributions: J.N. and A.G. designed the project; A.G., E.G., J.Y., T.C. and T.K. performed experiments and analyzed data; All authors contributed to the prepration of the manuscript.

Competing interests: The authors have no competing interests.

genes prolong the cardiac action potential. The clinical syndrome is classically defined by hypotensive syncopal episodes, but distinguishing between these spells and certain seizure auras with or without myoclonus can be difficult (7). Combined EEG/ECG studies confirm the high prevalence (33–44%) of cardiac arrhythmias in individuals with true epileptic seizures (7–11). Indeed, a presumptive clinical seizure phenotype was found in up to one-third of genotyped LQTS patients, including 22% of those with confirmed LQT1 mutations, suggesting that an LQT gene could underlie neuronal hyperexcitability (12). The simultaneous presence of seizures and LQTS in these individuals might also be coincidental, since there are multiple genetic and acquired etiologies for both epilepsy and LQTS. An important clue that they could be related arose from the initial observation that one gene for LQTS, encoding a cardiac voltage-gated sodium ion channel associated with ventricular fibrillation and sudden death (13,14), is co-expressed in certain limbic regions of brain such as the entorhinal cortex and amygdala (15). In these regions there are low thresholds for aberrant network synchronization where prolonged depolarization may also trigger primary brain seizures. Although no LQTS ion channel gene mediating fast membrane rhythmicity has been directly linked to a neurocardiac phenotype predisposing to SUDEP to date, a single ion channelopathy accounts for pleiotropic phenotypes in heart and brain in the Timothy Syndrome, in which a mutation of an L-type calcium channel gene underlies both cardiac arrhythmia and autism (6,16). Further, mutation of RyR2, an intracellular ryanodine receptor mediating calcium homeostasis in neurons and cardiomyocytes leads to both seizures and exercise-induced catecholaminergic polymorphic ventricular tachycardia (CPVT)(17).

Mutations in the *KCNQ1* gene at the LQT1 locus (11p15.5) underlie the most common form (approximately half of genotyped cases) of LQTS in the population (6). This gene encodes the α-subunit of the tetrameric voltage-gated potassium channel KvLQT1 (Kv7.1). LQT1 mutations decrease the slow repolarizing I_{KS} current, which causes the underlying cardiac phenotype (18–20). Two mouse models, each carrying a dominant point mutation in the *Kcnq1* gene found in LQT1 patients, reproduce the human cardiac LQT phenotype (21). They also display auditory defects, in accordance with the accepted expression pattern of *KCNQ1* in heart and auditory hair cells, but no epileptic phenotype was reported (21,22). Most studies of *KCNQ1* failed to find mRNA transcripts or KvLQT1 in the brain, precluding a role for this channel in the central nervous system (Table S1). Nevertheless, we reexamined this question because, if present in neural networks, arrhythmogenic cardiac mutations in this channel might also cause epileptiform changes in brain, thereby revealing a unifying cause of both idiopathic epilepsy and cardiac arrhythmia, as well as an identifiable risk factor for SUDEP.

RESULTS

KCNQ1 and *MinK* brain expression patterns

There are conflicting reports in the literature on whether mRNA for the ion channel KvLQT1 is expressed in the mammalian central nervous system (see Table S1). We confirmed the unequivocal presence of *KCNQ1* subunit mRNA in multiple regions of the developing and adult wildtype mouse and adult human brain by RT-PCR and localized the channel protein within the nervous system using two different subunit-specific polyclonal antibodies. Sequencing of PCR amplicons confirmed the expression of *KCNQ1* isoforms that lead to a functional channel protein in the heart, as well as of a previously undescribed transcript specific to the human central nervous system (Fig. 1A–C). We also confirmed the presence of mRNA transcripts of *MinK* (*KCNE1*), a known modulatory subunit of heart KCNQ1-containing channels, in multiple mouse and human brain regions (Fig. 2A–B). Expression of *MinK* was detected at three different stages of mouse development (Fig. 2A). Using a commercial α-subunit-specific antibody to KvLQT1, we confirmed the presence of the corresponding wild-type protein in the mouse brain and heart at the expected apparent molecular weight of 75 kDa

(Fig. 2C, Fig. S1A). We also confirmed the presence of MinK protein in hippocampus, cortex and heart, at the expected molecular weight of 15 kDa (Fig. 2D, Fig. S1B). The commercial antibody to MinK also detected a 90 kDa immunoreactive band in whole mouse brain, hippocampus and cortex (Fig. 2E, Fig. S1B). We postulated that this band represents a complex of a single KvLQT1 pore-forming α-subunit (75 kDa) and a single MinK subunit (15 kDa) that is not disrupted by heat and SDS. This was confirmed by co-immunoprecipitation, in which the 90 kDa band was detected by anti-MinK immunoblotting of brain lysate samples immunoprecipitated by either the KvLQT1 specific antibody or MinK antibody (Fig. 2F, Fig. S6C), consistent with previous reports (23,24).

Immunofluorescence revealed the regional localization pattern of KvLQT1 in the adult wildtype mouse brain (Fig. 3). We found prominent protein expression within hippocampal network pathways involved in epileptogenesis, including granule cells of the dentate gyrus, pyramidal cells of the CA1-3 regions, and hilar interneurons. We observed moderate to strong neuropil staining in the region of the mossy fiber pathway coursing from the hilus to CA3, but this labeling could be attributed to either granule cell mossy fiber axons or to CA3 pyramidal cell processes. We noted additional staining in neurons within most cortical layers, in thalamus, and in scattered glia-like cells within white matter tracts. KvLQT1-positive neurons also populated the medullary dorsal motor nucleus of the vagus and the nucleus ambiguus, brainstem centers contributing preganglionic parasympathetic innervation via the vagal nerve to the heart (Fig. 4A–C). No KvLQT1-positive cells were apparent in the intermediolateral columns of the thoracic spinal cord where preganglionic sympathetic neurons innervating the heart reside.

Cortical and cardiac abnormalities in mice with human LQTS mutations

We next analyzed mouse lines engineered to carry the orthologous point mutations in *Kcnq1* that underlie two human long QT syndromes (Fig. 5, Fig. S2). Mice carrying the *A340E* mutation (*A341E* in humans) in the S6 transmembrane helix model the Romano Ward syndrome (autosomal dominant form of familial LQTS with ventricular tachyarhythmias). Mice homozygous for *T311I* (*T312I* in humans) in the pore region display a complex phenotype of deafness and LQT intervals resembling patients with Jervell and Lange-Nielsen syndrome (autosomal recessive form of familial LQTS associated with deafness and tachyarrhythmias) (21). We examined cortical and cardiac rhythms in both mutant lines by simultaneously monitoring EEG and ECG in freely moving mice. Analysis of 19 mutant adult animals revealed that all displayed epileptiform EEG spike discharges and ECG arrhythmnias, in comparison with unaffected littermates, which exhibited only rare non-epileptiform waves or isolated cardiac premature ventricular contractions (PVCs) of no pathological significance (Table 1). Both knock-in lines exhibited frequent bilateral interictal epileptiform discharges represented by sharp waves, spikes, and polyspikes at an average rate of ~3 spikes/min. Although homozygous mutants displayed more cortical spikes than heterozygotes, this trend did not reach statistical significance between genotypes (ANOVA, $P = 0.27$). EEG abnormalities in the mutants also consisted of prolonged runs of focal slow waves, mainly in the temporal regions. We also observed a variety of aberrant ECG events (~1.5/min) not present in wildtype littermates (Table 1). Unlike recordings previously described in genetically identical but sedated mice (21,25), awake mutant mice displayed clear spontaneous cardiac rhythm disturbances, including atrial fibrillation, atrial flutter, premature ventricular contractions, and episodic atrio-ventricular conduction block (Figures S3–S5). Comparisons of standard ECG parameters for heart rate variability between homozygous mutants and wildtype controls sampled during 2 minute periods of inactivity revealed no significant differences (Table S2).

Dual simultaneous EEG/ECG recordings showed that interictal hypersynchronous cortical discharges often coincided with either prolongation of the cardiac RR interval (time between

two consecutive R waves) and premature ventricular contractions or asystole (Fig 7A). These patterns are consistent with autonomic instability and have been described in SUDEP patients (26) (Fig. 6A, Figures S3–S5 and Table 1). Cortical discharges also occured without concomitant arrythmia (Fig. 6B, Fig. S6). We analyzed the frequency of concurrent neurocardiac events to better evaluate a possible interaction between the observed EEG and ECG abnormalities. We found that about 24% of all cortical discharges were concurrent with ECG events, while approximately 62% of cardiac abnormalities occurred in association with epileptiform discharges. Therefore, although ECG abnormalities could occur in the absence of cortical discharges, the majority were coupled with abnormal synchronous EEG activity.

Epilepsy and SUDEP in LQTS mice

VideoEEG monitoring detected frequent partial and generalized seizures in all mutant animals but not in wildtype littermates. Two main seizure types were observed. The first was characterized by sudden arrest of activity, followed by tonic extension and whole body convulsive movements (Video S1). The EEG correlate was a pattern of bilateral rhythmic high-voltage sharp wave discharges evolving into a higher frequency rhythmic discharge (Fig. 7A). The second and more common type consisted of partial motor seizures characterized by behavioral arrest and subtle clonic movements of the jaw, head, limbs, or entire body (Video S2). The EEG correlate was low-voltage rhythmic slow activity interspersed with spike and slow-wave discharges coinciding with the clonic movements (Fig 7B). The prevalence of witnessed convulsive seizures was 33% in the heterozygous animals and 80% and 60% in *A340E* and *T311I* homozygous mice, respectively. Subtle partial seizures with EEG correlates were seen in all mutants, with a mean frequency reflecting the genotype (8.7, 4.7, and 0 per hour in *A340E* homozygotes, heterozygotes, and wildtype, respectively; and 9.7, 6, and 0 per hour in *T311I* homozygotes, heterozygotes, and wildtype, respectively). During peri-ictal and ictal states we observed a similar range of ECG abnormalities as those seen during inter-ictal periods.

Although *Kcnq1 A340E* and *T311I* mutant mice typically live into adulthood, prolonged monitoring resulted in the fortuitous capture of a terminal event. Over a period of several hours, a *T311I/T311I* homozygote showed frequent partial seizures with subtle behavioral manifestations evolving into electro-clinical non-convulsive status epilepticus. This period was characterized by profound bradycardia punctuated by frequent ventricular escape beats and runs of ventricular fibrillation. Electrographic seizure activity gradually evolved into a burst suppression-like pattern with concomitant severe cardiac depression (heart rate of 120–160 bpm) for many hours, electrocerebral silence, visibly shallow respirations, and ultimate cardiac arrest (Fig. 7C).

DISCUSSION

We localized KvLQT1, a principal myocardial potassium channel, in central neurons, and found that mice bearing human LQT1 mutations in this channel display seizures and malignant cardiac arrhythmias. Our study identifies mutation of *KCNQ1*, a previously unrecognized neuronal potassium channel in brain, as a cause of epilepsy and provides a neurobiological basis for seizures witnessed in humans bearing mutations in this gene. Since these mutations also cause life-threatening cardiac arrhythmias, they are a molecular risk factor for sudden death in epilepsy (SUDEP). The two mouse models with human LQT1 mutations define a candidate excitability-linked mechanism for SUDEP. Mutant KvLQT1 repolarization defects expressed within the forebrain and brainstem autonomic outflow pathway could compromise a direct relay between the epileptic brain and cardiac pacemaking. We observed brief seizures in both mutant knock-in strains and the majority of the events were similar to subtle human partial seizures. In the EEG, cortical discharges were often, but not always followed within

two hundred milliseconds by cardiac conduction disturbances. The high incidence of concurrent EEG/ECG events in the presence of either LQT mutation is consistent with an intermittant dysfunctional neurocardiac interplay, presumably under the influence of other extrinsic autonomic or humoral factors modulating brain excitability and cardiac pacemaking that maintain normal function until the onset of profound bradycardia, hypotension, and death following a prolonged seizure.

The presence of KvLQT1 in neurons within mouse vagal brainstem nuclei raises the possibility that this channelopathy may influence cardiorespiratory physiology. Along with parasympathetic slowing of the heart, the vagal nerve also controls motor tone in the upper airway and stimulates neurogenic pulmonary edema, a finding often reported at autopsy of SUDEP cases (4,27,28). It is therefore plausible that excitability defects in these efferent pathways depress respiration, contributing additional vulnerability during the post-ictal period. In our witnessed instance of SUDEP in a *T311I/T311I* mouse, there was a loss of brain wave activity and slowed respiration, followed by a progressive lethal bradycardia during the terminal event. This sequence mirrors that of the only reported human SUDEP case with simultaneous intracranial recording (29).

These findings establish the crucial role of *KCNQ1* in neuronal network synchronization and epileptogenesis. It is a member of the *KCNQ* gene family encoding five voltage-gated delayed rectifier K^+ channels (KCNQ1-5), four of which (KCNQ2-5) are also expressed in the brain. Interestingly, the hippocampal immunostaining pattern of KvLQT1 overlaps with networks expressing *KCNQ2* and *KCNQ3* proteins (Kv7.2 and Kv7.3 respectively), both of which are also linked to epilepsy by a variety of mutations in human and mouse (30,31). The KvLQT1 protein is a pore-forming α-subunit of a channel complex that co-assembles with the β-subunit encoded by *KCNE1* (MinK), but not any other member of the KCNQ family, forming a channel that generates the slow delayed rectifier potassium current (I_{KS}) in human cardiac myocytes. Functional effects of the *KCNQ1* mutations producing epilepsy in our models have been extensively studied in Xenopus oocytes where they exert dominant-negative suppression of outward potassium currents when co-expressed with wildtype KvLQT1 subunits (18,19). The presence and co-assembly of KvLQT1 and MinK in mouse brain (Fig 2) suggests that the protein may modulate neuronal excitability as a KvLQT1/MinK complex as I_{KS} does in heart.

The molecular consequences of *KCNQ1* mutations fall into several categories: impaired channel assembly and trafficking, dysfunctional ion channel gating, altered interaction with second messengers, and inhibition of binding to regulatory proteins. Almost 300 human *KCNQ1* mutations have been identified to date and the majority of variants in the pore region or voltage sensor lead to loss of function and LQTS with or without congenital deafness, a few gain of function mutations are associated with familial atrial fibrillation or short QT syndrome (32,33). Individuals with truncations and point mutations in the C terminus are either asymptomatic or exhibit borderline QT prolongation and a mild clinical phenotype (34). The imperfect correlation between channel physiology and the clinical phenotype in different tissues suggests the possibility that not all human *KCNQ1* mutations may give rise to an epileptic phenotype, or may do so only on permissive genomic backgrounds.

The difficulty of distinguishing clinically between syncopy and seizure represent a major challenge to the accuracy of genotype to phenotype correlations in LQT/epilepsy patients. Considering that the most common ictal events observed in the mouse LQT1 models were partial seizures lasting less than ten seconds without prominent clonic movements, it is likely that infrequent subclinical seizure activity in humans with *KCNQ1* mutations is often undetected. This is consistent with the experience in epilepsy monitoring units where very brief partial, temporal lobe EEG seizures in otherwise healthy individuals may go unnoticed (35).

Although the detection of individuals with epilepsy at risk for SUDEP represents a major clinical challenge, the prevalence of occult cardiac arrhythmia in idiopathic epilepsy is understudied and potentially larger than currently assumed. Russell commented in 1906 that "…cardiac arrest does occur in some cases of epilepsy and … may be far commoner than is suspected. If observations were made on the pulse at the onset of fits by those whose work brings them into contact with epileptic patients in considerable numbers, it would soon be established whether such cardiac arrest be of occasional or of frequent occurrence" (5). Our literature review of the past 30 years yielded over 80 case reports of seizures associated with cardiac arrythmia, and 47% of these were associated with asytole. A recent report on prolonged ambulatory ECG monitoring in a small group of epilepsy patients revealed that 21% had bradycardia associated with seizures, and 3 of 4 of these showed potentially fatal asystole (36). Our two mouse models recapitulated the association of epilepsy and a spectrum of cardiac arrythmias, including SUDEP, observed repeatedly in clinical settings and will be useful in the search for therapies to prevent SUDEP. Adrenergic β blockade and implantable pacemakers may prove useful for gene-directed prophylaxis (37–39). Finally, mutations in other LQT channels and their interacting subunits expressed in the brain may also cause epilepsy with an increased risk of SUDEP. Here, we suggest that the practicing clinician consider the neurocardiological ramifications of idiopathic epilepsies. Comprehensive clinical and genotypic LQT risk profiling in patients with idiopathic seizure disorders, followed by appropriate therapy, may reduce the likelihood of fatal arrhythmia in these individuals.

MATERIALS AND METHODS

Detection of *KCNQ1* and *MinK* brain expression

Mouse brain and heart isolation—Mice were euthanized by cervical dislocation. Whole brain and heart were promptly removed under sterile, RNA-ase free conditions, dissected, and frozen immediately on dry ice.

Human brain tissue—Deidentified frozen human postmortem brain tissue samples were obtained from the Department of Pathology (Texas Children's Hospital).

Brain tissue RNA extraction—Tissues were homogenized with a Tissue Tearor and RNA was extracted using Trizol (Life Technologies) following the manufacturer's standard protocol.

RT-PCR—Gene specific primers were designed to unique regions of human (Genbank accession AJ006345) and mouse (accession AJ251835) *KCNQ1* isoforms and human (accession NM_000219) and mouse (accession NM_008424) *MinK* transcripts. Forward primers for detection of the human *KCNQ1* isoforms 1 and 2 were amplified across exons 1a-1/2 (5′-CGCGTCTACAACTTCCTCG-3′) and exons 1b-1/2 (5′-TTTCTGGCTCTCGGGAATTT-3′), respectively. The identical reverse primer was used to amplify both human *KCNQ1* isoforms (5′-ATCCAGAAGAGAGTCCCCGT-3′). Mouse *KCNQ1* primers were used to amplify across exons 1a – 3/4 (5′-GGGTTGGAAGTGTTTCGTGT-3′ and 5′-CGGATACCCCTGATAGCTGA-3′. The forward primer for the detection of human *MinK* transcripts targeted the 5′ end of the transcript (5′-GAGGATCCATTGGAGGAAGG-3′) and the reverse primer was positioned in the coding exon (5′-AGGCCTTGTCCTTCTCTTGC-3′, 388bp). An identical strategy was employed in designing the detection primers for mouse *MinK* transcripts (forward; 5′-CTACCTCTGCACCGTCCATC-3′; reverse; 5′-AGCAAGCTCTGAAGCTCTCC-3′). PCR amplifications used 30 cycles with one minute extension time. RT-PCR was performed using SuperScriptIII™ RT-PCR System (Invitrogen, Life Technologies) according to the supplied protocol. An aliquot of the PCR amplification was analyzed on a 2% agarose gel and the products were purified using the QIAquick PCR purification kit (Qiagen) and submitted for

sequencing. Amplicon sequences were compared to those in GenBank to insure accurate and appropriate amplification of the desired gene.

KvLQT1 and MinK protein expression—Whole mouse brain, cortex, hippocampus and heart were extracted, flash frozen on dry ice, and subsequently homogenized on ice with a Tissue Tearor in RIPA buffer containing protease and phosphatase inhibitors (Santa Cruz). Total protein concentrations in the cell lysate were determined using the Bio-Rad Protein Assay (Bio-Rad). Forty micrograms of each sample was separated on 8% Tris–glycine SDS polyacrylamide gels, analyzed by Western blot (WB) using rabbit polyclonal anti-KvLQT1 antibody (1:200 in vehicle; Millipore) or anti-MinK antibody (1:250 in vehicle, Millipore) HRP-tagged goat anti-rabbit F(ab′)2 secondary antibody (1:500 dilution in vehicle, Molecular Probes) and subsequently detected with a commercial chemiluminescent substrate (SuperSignal; Pierce Chemical). For immunoprecipitation experiments, cell lysates were diluted to 1 mg/mL and each 1 mL sample was precleared for 1 h with 30 μL of protein A-Sepharose (Pharmacia) and incubated overnight with 5 μg of anti-KvLQT1 antibody (Sigma) or anti-MinK (Millipore). All incubations were performed at 4 °C with constant rotation. Antibody-bound protein complexes were captured by the addition of 30 μL of protein A-Sepharose and incubated for another 2 h. Protein A-Sepharose was pelleted by centrifugation and the immunoprecipitated protein complexes were eluted using SDS-PAGE sample buffer prior to SDS-PAGE and Western blotting as described above. The antigenic regions of both commercial antibodies target unique sequences in the C-terminus of KvLQT1 not found in any other voltage-dependent potassium channel (Fig. S8). Specific immunoreactivity for KvLQT1 was confirmed in transiently transfected HEK293 cells (Fig. S9).

Immunofluorescence in mouse brain sections

Preparation of brain sections—C57BL/6J mice (2–3 months old) were perfused intracardially with PBS and fixed with 4% paraformaldehyde in PBS. Brains were removed, cryoprotected for 1–2 days at 4°C in 30% sucrose in PBS, frozen in embedding medium, and cut into 20 μm sections using a cryostat maintained at −20°C. The sections were then directly mounted on slides for processing.

Immunofluorescence—The brain sections were rinsed three times in PBS and incubated for 1 hour in antibody vehicle (10% BSA, 0.3% Triton X-100 in PBS). Next, the sections were incubated overnight (15–20 hours) at room temperature with affinity purified rabbit polyclonal anti-KvLQT1 antibody (1:250 dilution in vehicle; Millipore). Subsequently, sections were washed three times in antibody vehicle and incubated for one hour in Alexa Fluor 488 goat anti-rabbit F(ab′)2 secondary antibody (1:1000 dilution in vehicle, Molecular Probes). Control experiments performed by incubating slices with only secondary antibodies showed an absence of background staining. Finally, sections were rinsed once in vehicle and twice in PBS and then air dried at room temperature for 30 minutes. Once dry, the slides were cover-slipped and mounted using ProLong Gold anti-fade reagent with DAPI (Invitrogen). Images were captured using an Olympus IX71 microscope and SimplePCI software. Whole images were colored to reflect the fluorphore used and were contrast adjused using Adobe Photoshop Elements 2.0.

Simultaneous EEG and ECG Recordings

Kcnq1 knock-in mouse lines and littermate wildtype control mice ranging from 23 days to 7 months of age were handled in accordance with the NIH Guide for the Care and Use of Laboratory Animals and surgically implanted under avertin anesthesia with a microminiature connector attached to silver wire electrodes (0.005-inch diameter). EEG electrodes were positioned through cranial burr holes overlying the cortical surface in the subdural space over the brain, and two ECG electrodes were implanted subcutaneously by trocar on either side of the thorax and secured with sutures. After at least one day of post-surgical recovery,

simultaneous cortical EEG and ECG activity was recorded in freely moving mice monitored for periods of 3–24 hours per day over multiple days using a digital video monitoring system (Stellate Systems, Harmonie software, versions 5.0b and 6.1c). Each animal was monitored by EEG/ECG for an average of 35 hours. The recordings were collected from five *A340E/A340E* mice, three *A340E/+* mice, four A340E wildtype littermates, five *T311I/T311I* mice, six *T311I*/+ mice and three T311I wildtype littermates. Video-EEG and ECG recordings were analyzed by an individual blinded to the genotype while ensuring that comparisons in each animal displayed similar states of arousal and background activity. The behavioral phenotype of the recorded mice was assessed by reviewing the digital video associated with each electrographic epoch.

The ECG arrhythmias were categorized according to established criteria (21,25,40) and in consultation with a cardiologist board-certified in cardiac electrophysiology (RF). EEG abnormalities were defined according to widely accepted standards (41,42). Briefly, the EEG waveforms were classified as epileptiform if (i) the waveforms assumed any one of these configurations: a spike, a spike and slow wave complex, a sharp wave or a sharp and slow wave complex; (ii) the epileptic spike or sharp wave was distinct and clearly defined against the baseline background. The waveform was classified as a spike if the duration was 20–70msec and as a sharp wave if the duration was 70–200 msec. EEG waveforms were classified as non-epileptic sharp transients in accord with widely accepted criteria if (i) they were sharply contoured waveforms that appeared as part of the background, (ii) they appeared only once in the entire recording segment, and (iii) the configuration, duration, and phase criteria did not comply with that of a definite epileptic discharge.

Statistical analysis

Absolute counts of EEG and ECG events were obtained by examining two separate 1-hour recordings from six animals per mutant genotype (homzygotes and heterozygotes) and from four *A340E* and three *T311I* corresponding wildtype littermates. The EEG and ECG abnormalities were scored as concurrent if the ECG event occurred within 200 milliseconds of the EEG ictal or inter-ictal discharge. Prolonged runs of atrial fibrillations, ventricular fibrillations or other cardiac event clusters, observed commonly in both mouse lines, were counted as a single event. Statistical analysis of EEG and ECG events was done with Microsoft Excel 2007 Analysis ToolPak (Microsoft) employing ANOVA to assess differences between event frequencies between genotypes in both lines.

Supplementary Material

Refer to Web version on PubMed Central for supplementary material.

Acknowledgments

We thank K. Pfeifer (NIH) for the gift of mutant mouse strains and both R. Friedman and D. L. Burgess for helpful assistance. Funding: NIH 5K08NS47304 (AG), NIH NS29709 (JLN), American Heart Association Postdoctoral Fellowship (EG), Dana Foundation (JLN), and the Blue Bird Circle Foundation for Pediatric Neurology Research.

References and Notes

1. Nashef L, Hindocha N, Makoff A. Risk factors in sudden death in epilepsy (SUDEP): the quest for mechanisms. Epilepsia 2007;48:859–871. [PubMed: 17433051]
2. Tomson T, Nashef L, Ryvlin P. Sudden unexpected death in epilepsy: current knowledge and future directions. Lancet Neurology 2008;7:1021–1031. [PubMed: 18805738]
3. Hitiris N, Suratman S, Kelly K, Stephen LJ, Sills GJ, Brodie MJ. Sudden unexpected death in epilepsy: a search for risk factors.[see comment]. Epilepsy & Behavior 2007;10:138–141. [PubMed: 17196884]

4. Stollberger C, Finsterer J. Cardiorespiratory findings in sudden unexplained/unexpected death in epilepsy (SUDEP). Epilepsy Research 2004;59:51–60. [PubMed: 15135167]
5. Russell AE. Cessation of the pulse during the onset of epileptic fits. Lancet 1906;10:152–154.
6. Goldenberg I, Moss AJ. Long QT syndrome. Journal of the American College of Cardiology 2008;51:2291–2300. [PubMed: 18549912]
7. McKeon A, Vaughan C, Delanty N. Seizure versus syncope.[erratum appears in Lancet Neurol. 2006 Apr;5(4):293]. Lancet Neurology 2006;5:171–180. [PubMed: 16426993]
8. Opherk C, Coromilas J, Hirsch LJ. Heart rate and EKG changes in 102 seizures: analysis of influencing factors. Epilepsy Research 2002;52:117–127. [PubMed: 12458028]
9. Zijlmans M, Flanagan D, Gotman J. Heart rate changes and ECG abnormalities during epileptic seizures: prevalence and definition of an objective clinical sign. Epilepsia 2002;43:847–854. [PubMed: 12181003]
10. Nei M, Ho RT, Sperling MR. EKG abnormalities during partial seizures in refractory epilepsy. Epilepsia 2000;41:542–548. [PubMed: 10802759]
11. Britton JW, Ghearing GR, Benarroch EE, Cascino GD. The ictal bradycardia syndrome: localization and lateralization. Epilepsia 2006;47:737–744. [PubMed: 16650140]
12. Johnson JN, Hoffman N, Haglund CM, Cascino GD, Wilde AAMJ. Ackerman Identification of a possible pathogenic link between congenital long QT syndrome and epilepsy. Neurology. Nov 26;2008
13. Wang Q, Shen J, Splawski I, Atkinson D, Li Z, Robinson JL, Moss AJ, Towbin JA, Keating MT. SCN5A mutations associated with an inherited cardiac arrhythmia, long QT syndrome. Cell 1995;80:805–811. [PubMed: 7889574]
14. Chen Q, Kirsch GE, Zhang D, Brugada R, Brugada J, Brugada P, Potenza D, Moya A, Borggrefe M, Breithardt G, Ortiz-Lopez R, Wang Z, Antzelevitch C, O'Brien RE, Schulze-Bahr E, Keating MT, Towbin JA, Wang Q. Genetic basis and molecular mechanism for idiopathic ventricular fibrillation. Nature 1998;392:293–296. [PubMed: 9521325]
15. Hartmann HA, Colom LV, Sutherland ML, Noebels JL. Selective localization of cardiac SCN5A sodium channels in limbic regions of rat brain. Nature Neuroscience 1999;2:593–595.
16. Splawski I, Timothy KW, Sharpe LM, Decher N, Kumar P, Bloise R, Napolitano C, Schwartz PJ, Joseph RM, Condouris K, Tager-Flusberg H, Priori SG, Sanguinetti MC, Keating MT. Ca(V)1.2 calcium channel dysfunction causes a multisystem disorder including arrhythmia and autism. Cell 2004;119:19–31. [PubMed: 15454078]
17. Lehnart SE, Mongillo M, Bellinger A, Lindegger N, Chen BX, Hsueh W, Reiken S, Wronska A, Drew LJ, Ward CW, Lederer WJ, Kass RS, Morley G, Marks AR. Leaky Ca2+ release channel/ryanodine receptor 2 causes seizures and sudden cardiac death in mice. Journal of Clinical Investigation 2008;118:2230–2245. [PubMed: 18483626]
18. Westenskow P, Splawski I, Timothy KW, Keating MT, Sanguinetti MC. Compound mutations: a common cause of severe long-QT syndrome. Circulation 2004;109:1834–1841. [PubMed: 15051636]
19. Wang Z, Tristani-Firouzi M, Xu Q, Lin M, Keating MT, Sanguinetti MC. Functional effects of mutations in KvLQT1 that cause long QT syndrome. Journal of Cardiovascular Electrophysiology 1999;10:817–826. [PubMed: 10376919]
20. Wang Q, Curran ME, Splawski I, Burn TC, Millholland JM, VanRaay TJ, Shen J, Timothy KW, Vincent GM, de Jager T, Schwartz PJ, Towbin JA, Moss AJ, Atkinson DL, Landes GM, Connors TD, Keating MT. Positional cloning of a novel potassium channel gene: KVLQT1 mutations cause cardiac arrhythmias. Nature Genetics 1996;12:17–23. [PubMed: 8528244]
21. Casimiro MC, Knollmann BC, Yamoah EN, Nie L, Vary JC Jr, Sirenko SG, Greene AE, Grinberg A, Huang SP, Ebert SN, Pfeifer K. Targeted point mutagenesis of mouse Kcnq1: phenotypic analysis of mice with point mutations that cause Romano-Ward syndrome in humans. Genomics 2004;84:555–564. [PubMed: 15498462]
22. Kubisch C, Schroeder BC, Friedrich T, Lutjohann B, El-Amraoui A, Marlin S, Petit C, Jentsch TJ. KCNQ4, a novel potassium channel expressed in sensory outer hair cells, is mutated in dominant deafness. Cell 1999;96:437–446. [PubMed: 10025409]

23. Calloe K, Nielsen MS, Grunnet M, Schmitt N, Jorgensen NK. KCNQ channels are involved in the regulatory volume decrease response in primary neonatal rat cardiomyocytes. Biochimica et Biophysica Acta 2007;1773:764–773. [PubMed: 17442416]
24. Finley MR, Li Y, Hua F, Lillich J, Mitchell KE, Ganta S, Gilmour RF Jr, Freeman LC. Expression and coassociation of ERG1, KCNQ1, and KCNE1 potassium channel proteins in horse heart. American Journal of Physiology - Heart & Circulatory Physiology 2002;283:H126–138. [PubMed: 12063283]
25. Casimiro MC, Knollmann BC, Ebert SN, Vary JC Jr, Greene AE, Franz MR, Grinberg A, Huang SP, Pfeifer K. Targeted disruption of the Kcnq1 gene produces a mouse model of Jervell and Lange-Nielsen Syndrome. Proceedings of the National Academy of Sciences of the United States of America 2001;98:2526–2531. [PubMed: 11226272]
26. Nei M, Ho RT, Abou-Khalil BW, Drislane FW, Liporace J, Romeo A, Sperling MR. EEG and ECG in sudden unexplained death in epilepsy. Epilepsia 2004;45:338–345. [PubMed: 15030496]
27. Fontan JJ, Diec CT, Velloff CR. Bilateral distribution of vagal motor and sensory nerve fibers in the rat's lungs and airways. American Journal of Physiology - Regulatory Integrative & Comparative Physiology 2000;279:R713–728.
28. Liu S, Kuo HP, Sheppard MN, Barnes PJ, Evans TW. Vagal stimulation induces increased pulmonary vascular permeability in guinea pig. American Journal of Respiratory & Critical Care Medicine 1994;149:744–750. [PubMed: 7906995]
29. Bird JM, Dembny KAT, Sandeman D, Butler S. Sudden Unexplained Death in Epilepsy: An Intracranially Monitored Case. Epilepsia 1997;38(Suppl 11):S52–S56. [PubMed: 9092961]
30. Singh NA, Westenskow P, Charlier C, Pappas C, Leslie J, Dillon J, Anderson VE, Sanguinetti MC, Leppert MF. Consortium, KCNQ2 and KCNQ3 potassium channel genes in benign familial neonatal convulsions: expansion of the functional and mutation spectrum. Brain 2003;126:2726–2737. [PubMed: 14534157]
31. Singh NA, Otto JF, Dahle EJ, Pappas C, Leslie JD, Vilaythong A, Noebels JL, White HS, Wilcox KS, Leppert MF. Mouse models of human KCNQ2 and KCNQ3 mutations for benign familial neonatal convulsions show seizures and neuronal plasticity without synaptic reorganization. J Physiol 2008;586:3405–3423. [PubMed: 18483067]
32. Peroz D, Rodriguez N, Choveau F, Baro I, Merot J, Loussouarn G. Kv7.1 (KCNQ1) properties and channelopathies. Journal of Physiology 2008;586:1785–1789. [PubMed: 18174212]
33. Chen YH, Xu SJ, Bendahhou S, Wang XL, Wang Y, Xu WY, Jin HW, Sun H, Su XY, Zhuang QN, Yang YQ, Li YB, Liu Y, Xu HJ, Li XF, Ma N, Mou CP, Chen Z, Barhanin J, Huang W. KCNQ1 gain-of-function mutation in familial atrial fibrillation. Science 2003;299:251–254. [PubMed: 12522251]
34. Haitin Y, Attali B. The C-terminus of Kv7 channels: a multifunctional module. Journal of Physiology 2008;586:1803–1810. [PubMed: 18218681]
35. Zangaladze A, Nei M, Liporace JD, Sperling MR. Characteristics and clinical significance of subclinical seizures. Epilepsia 2008;49:2016–2012. [PubMed: 18503561]
36. Rugg-Gunn FJ, Simister RJ, Squirrell M, Holdright DR, Duncan JS. Cardiac arrhythmias in focal epilepsy: a prospective long-term study.[see comment]. Lancet 2004;364:2212–2219. [PubMed: 15610808]
37. Berul CI. Congenital long-QT syndromes: who's at risk for sudden cardiac death?[comment]. Circulation 2008;117:2178–2180. [PubMed: 18443247]
38. Goldenberg I, Moss AJ, Peterson DR, McNitt S, Zareba W, Andrews ML, Robinson JL, Locati EH, Ackerman MJ, Benhorin J, Kaufman ES, Napolitano C, Priori SG, Qi M, Schwartz PJ, Towbin JA, Vincent GM, Zhang L. Risk factors for aborted cardiac arrest and sudden cardiac death in children with the congenital long-QT syndrome.[see comment]. Circulation 2008;117:2184–2191. [PubMed: 18427136]
39. Roden DM. Clinical practice. Long-QT syndrome.[see comment]. New England Journal of Medicine 2008;358:169–176. [PubMed: 18184962]
40. Isselbacher, KJ.; Braunwald, E.; Willson, JD.; Martin, JB.; Fauci, AS.; Kasper, DL. Harrison's Principles of Internal Medicine. McGraw Hill Inc; New York: 1994.

41. Niedermeyer, E.; Lopes Da Silva, F. Electroencephalography. Basic Principles, Clinical Applications, and Related Fields. Williams & Wilkins; Baltimore, MD, USA: 1998.

42. Fisch, BJ. Fisch and Spehlmann's EEG Primer: Basic Principles of Digital and Analog EEG. Elsevier Science Pub Co; Amsterdam. The Netherlands: 1999.

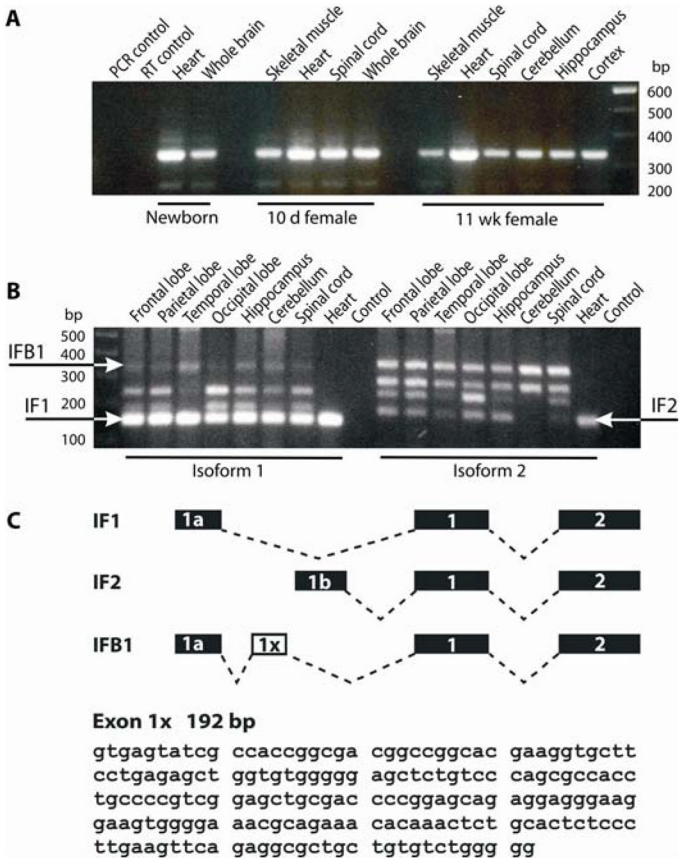

Figure 1. *KCNQ1* RNA transcripts are present in the mouse and human brain

(A) RT-PCR with primers targeting the 5′ end of the channel revealed *Kcnq1* mRNA transcripts in the heart and brain of a newborn mouse and multiple regions of the brain and heart of 10 day old pup and 11 week old adult mouse.

(B) RT-PCR of adult human brain with primers targeting the 5′ end of the *KCNQ1* mRNA reveals the presence of the functional isoforms A (IF1; 151 bp) and B (IF2; 162 bp) of *KCNQ1* in multiple regions of the brain and heart. A previously undescribed brain isoform (IFB1; 344 bp) was also detected in human brain.

(C) Schematic depiction of the alternative splicing of the 5′ end of *KCNQ1* transcripts. The transcripts for IsoA and IsoB forms have either exon 1 or exon 2 in the 5′ end, respectively. Sequencing of the novel brain isoform (IFB1) revealed the presence of a 192 bp exon (designated exon 1×) occurring immediately following exon 1. The nucleotide sequence of exon 1× is shown.

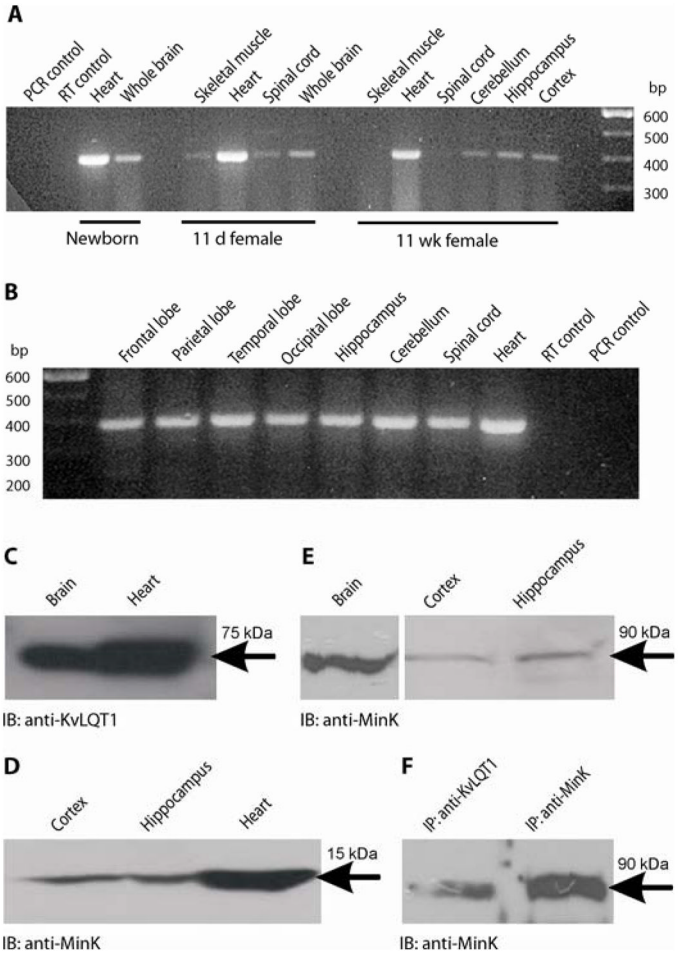

Figure 2. *MinK* RNA transcripts and protein are present in the brain and associate with KvLQT1

(A) RT-PCR with primers targeting the 5′ end of the murine *Kcne1* (MinK, Isk) transcript revealed the presence of *Kcne1* in the heart and brain of newborn mouse and in the brain, heart and skeletal muscle of an 11-day-old pup and 11-week-old adult mouse (393 bp).

(B) RT-PCR of adult human brain with primers targeting the 5′ end of the channel reveals the presence of *KCNE1* transcripts in multiple regions of the human brain and heart (388 bp).

(C) KvLQT1 protein subunits in the mouse brain. Immunoreactive bands with apparent molecular weight of ~75 kDa corresponding to murine KvLQT1 pore-forming α-subunits were detected in protein lysates of mouse brain and heart by Western immunoblotting (IB) with the polyclonal antibody to KvLQT1.

(D) MinK protein subunits in the mouse cortex, hippocampus and heart. Immunoreactive bands with apparent molecular weight of ~15 kDa corresponding to murine MinK subunits were detected in protein lysates of mouse cortex, hippocampus and heart by Western immunoblotting with the polyclonal antibody to MinK.

(E) Immunoreactive bands at ~90 kDa were detected in protein lysates of mouse whole brain, cortex and hippocampus using the antibody to MinK.

(F) Immunoreactive bands at ~90 kDa were detected in co-immunoprecipitates (IP) of mouse whole brain with antibodies to KvLQT1 and MinK, followed by immunoblotting with the antibody to MinK.

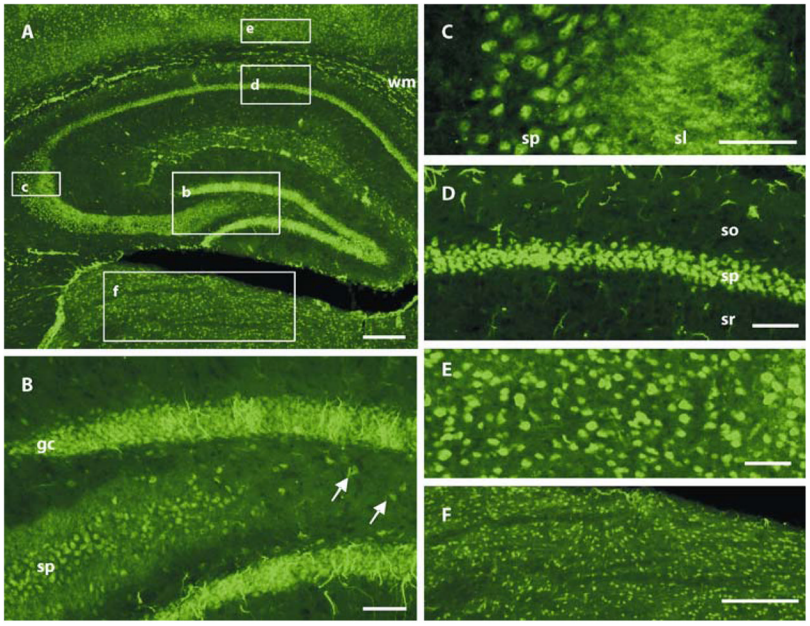

Figure 3. KvLQT1 immunoreactivity is distributed throughout regions important for epileptogenesis in the adult mouse brain

(A) We observed moderate to strong KvLQT1 immunoreactivity in the somata of cells in the hippocampal formation, including pyramidal neurons in CA1–CA3, granule cells of the dentate gyrus, and hilar interneurons. KvLQT1 antibody also labeled a majority of somata in the neocortex and thalamus, as well as glia-like processes in subcortical white matter tracts (*wm*) and the dentate granule cell layer. Moderate to strong neuropil staining was evident in the stratum lucidum (*sl*) where CA3 pyramidal cell apical dendrites and granule cell mossy fibers reside. *Boxes* correspond to regions shown at higher magnification in *B-F*.

(B) Detailed view of KvLQT1 staining in the dentate gyrus/hilar region, showing the CA3 pyramidal cell (*sp*) layer of the hippocampus, the granule cell (*gc*) layer of the dentate gyrus, and hilar interneurons (*arrows*). We observed intense staining of conspicuous processes that emanated from the granule cell layer and resembled type 1 radial glia-like cells.

(C) High magnification view of the hippocampal CA3 region showing strong staining of somata in the pyramidal cell layer and neuropil staining in stratum lucidum. Staining in stratum lucidum could be attributable to granule cell mossy fiber axons or CA3 pyramidal cell apical dendrites.

(D) A detailed view of the CA1 pyramidal cell layer showing strong KvLQT1 somatic staining.

(E) KvLQT1-labeled cells in deep neocortical layers..

(F) Enlarged view of staining of KvLQT1 in neuronal soma in the dorsal thalamus. so, stratum oriens; sr, stratum radiatum. Scale bars: a, f, 200 μm; b–e, 50 μm.

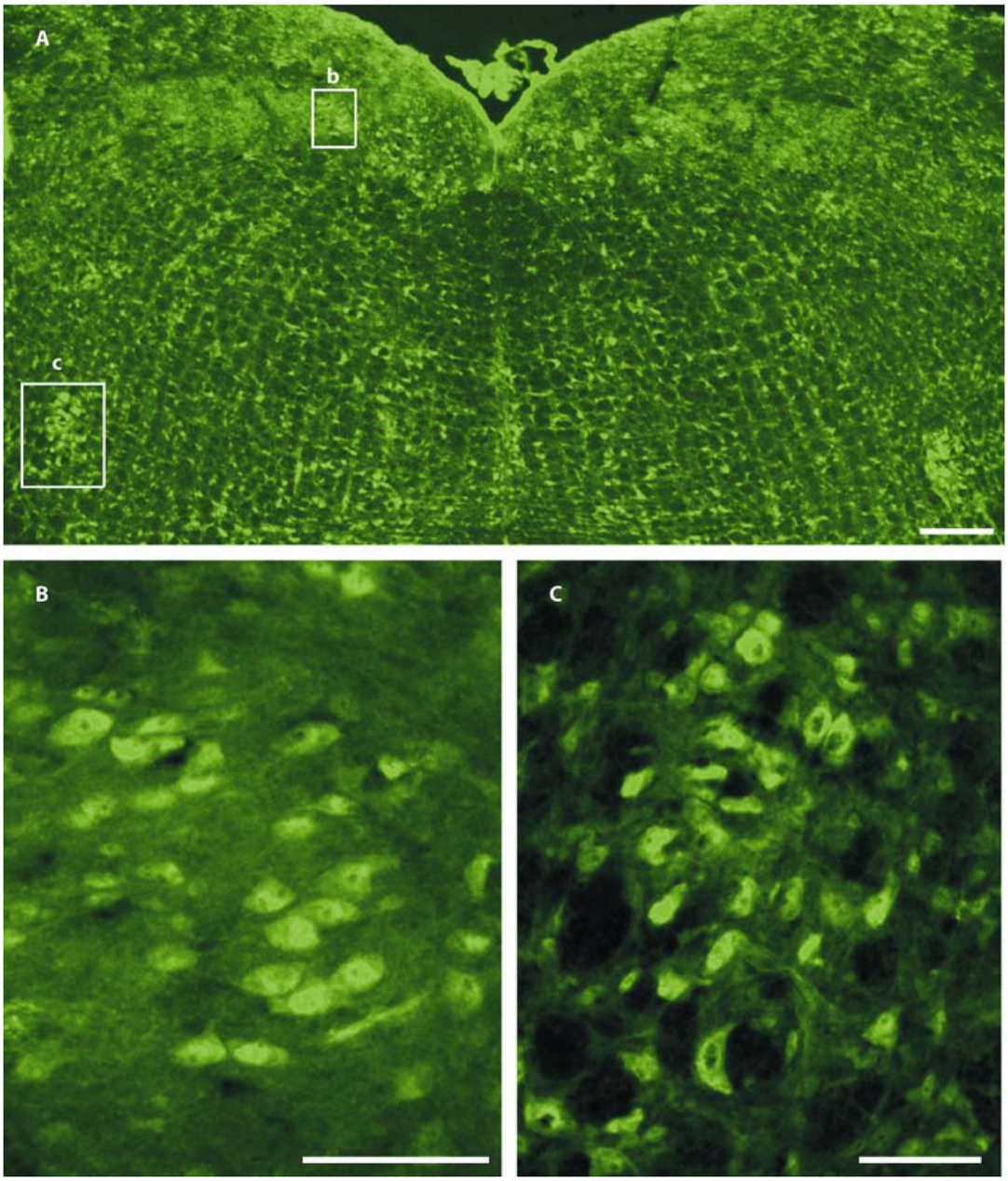

Figure 4. Distribution of KvLQT1 immunoreactivity in brainstem regions in the adult mouse brain

(A) Coronal sections of the medulla oblongata, KvLQT1 immunofluorescence was strong in somata of cardiac-related nuclei, including the dorsal motor nucleus of the vagus and the nucleus ambiguus, which are *boxed* and shown at higher magnification in *B* and *C*, respectively.

(B) High magnification view of KvLQT1 somatic staining in the dorsal motor nucleus of the vagus.

(C) High magnification view of KvLQT1 somatic staining in the nucleus ambiguus. Scale bars: a, 200 μm; b, c, 50 μm.

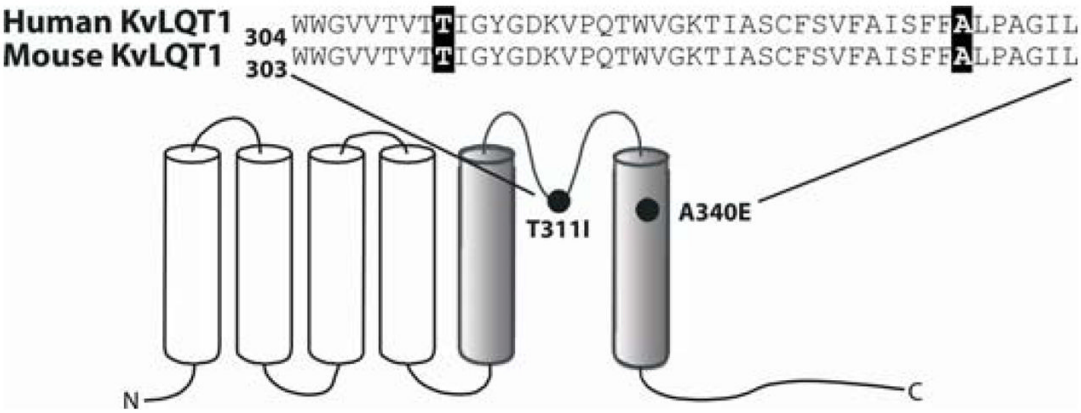

Figure 5.

Schematic diagram of the KvLQT1 α-subunit showing the location of the LQT1 mutations. A single six transmembrane diagram of KvLQT1 subunit showing the location of the two human mutations studied in the mutant mouse models (black circles; T311I and A340E). The aligned sequence of the highly conserved pore region of the human and mouse channel is shown.

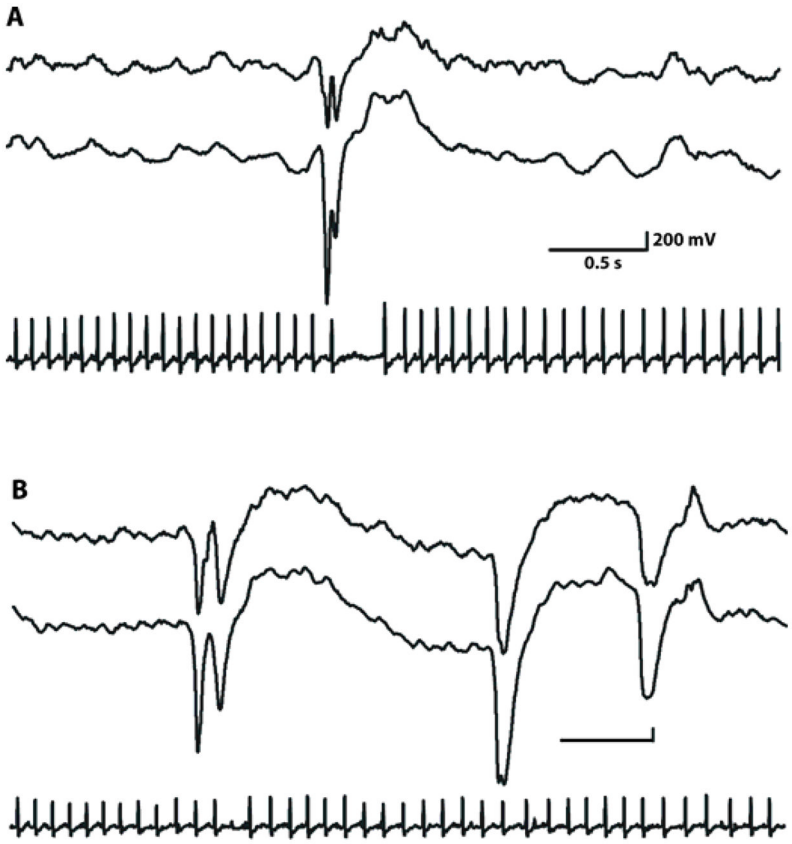

Figure 6. Aberrant brain-heart events in *Kcnq1* mutant mice during interictal discharges and cortical seizures

A) EEG recordings show frequent bilateral interictal discharges over temporal cortical regions of A340I homozygote with concomitant AV conduction block following P wave in ECG tracing.

B) Representative example of the intermittent nature of cortical-cardiac cycle events in KvLQT1 mutant mice. Cortical EEG discharges sometimes but not always coincided with cardiac events (Table 1). Here, ECG events occur concurrently with the two initial EEG ictal spikes but not with the third. The scale bar is the same in both *A* and *B*.

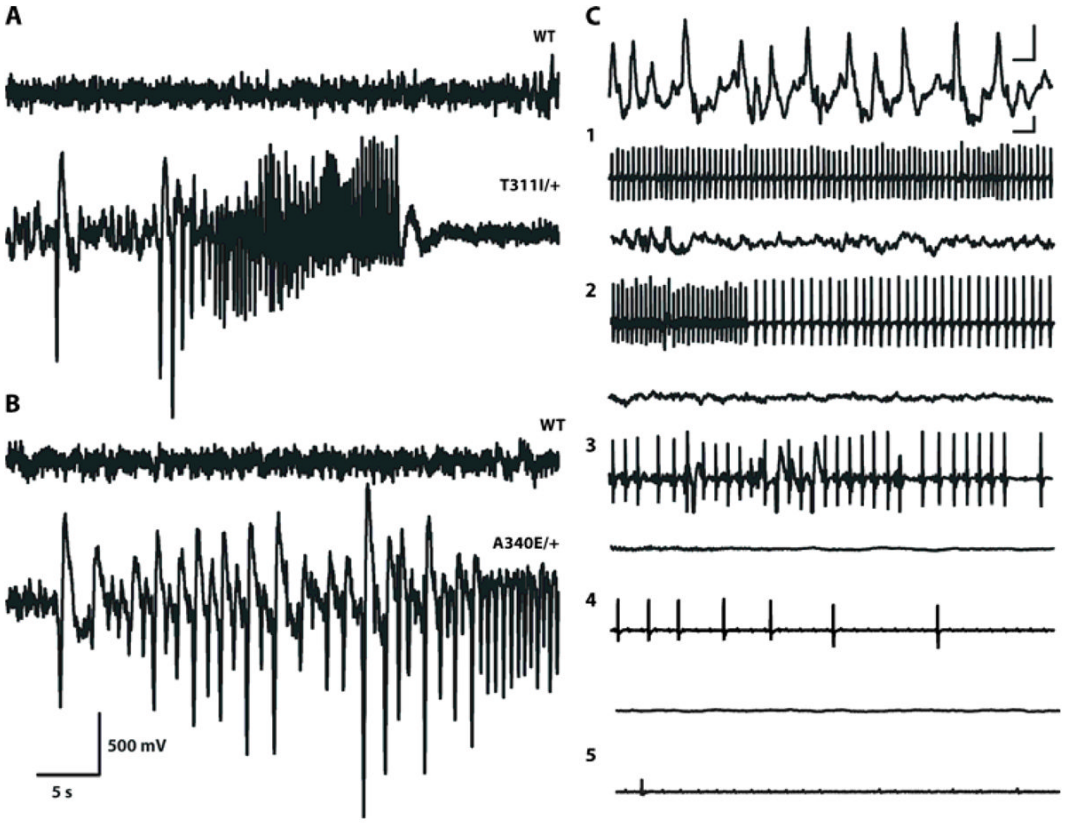

Figure 7. Mice with mutations in KvLQT1 have seizures and sudden death

(A) Representative EEG tracing of a wild-type littermate (top) and a *T311I* heterozygous mouse (bottom) at the onset of a spontaneous convulsive seizure. Remainder of seizure recorded with 4 electrode EEG montage is shown in Video S1.

(B) Representative EEG tracing of a wild-type littermate (top) and a *A340E* heterozygous mouse (bottom) showing onset of a spontaneous subtle partial seizure. Remainder of the seizure recorded with 4 electrode EEG montage is shown in Video S2.

The scale bar is the same for both *A* and *B*.

(C) Sequential EEG-ECG tracings recorded at various stages (1–5) during a terminal seizure in *T311I/T311I* mutant. Upper traces, unilateral cortical EEG activity, lower traces, ECG. The scale bars in both the EEG and ECG traces are 0.5 s and 200 mV.

Table 1

Summary of the number of EEG and ECG abnormalities detected in the *A340E* and *T311I* cohort

The data reprsent the mean number of abnormalities given as mean ± SEM obtained from represenntative animals from two sepearate one-hour recodings, evaluated by a person blinded to the genotype of the animal.

Mouse line (n)	Total Interictal EEG abnormalities (per hour)	Total Interictal ECG abnormalities (per hour)*	Concurrent EEG and ECG abnormalities (per hour)	Percentage of total EEG events with concurrent ECG event (concurrent EEG+ECG/total EEG)	Percentage of total ECG events with concurrent EEG event (concurrent EEG+ECG/total ECG)	Partial seizures (per hour)	Convulsive seizures**
A340E/A340E (3)	230.0±51.7	106.0±27.0	74.6±37.3	30.1±10.3	62.9±19.3	8.7±0.9	4
A340E/+ (3)	130.8±42.3	68.6±18.2	21.0±15.0	12.3±5.8	33.3±24.5	4.7±0.9	1
A340E wildtype (4)	2±0.72***	0.9±0.16 ****	0	0	0	0	0
T311I/T311I (3)	278.5±76.7	101.7±41.6	74.7±37.3	23.6±6.7	66.5±11.6	9.7±0.9	3
T311I/+ (3)	177.3±9.7	65.0±21.6	53.6±17.4	29.3±8.7	83.5±1.5	6±1	2
T311I wildtype (3)	2.5±1.74***	1.4±0.9 ****	0	0	0	0	0

* The motion artefact prevented accurate assessement of associated ECG abnormalities during partial and convulsive seizures.

** The stochastic character of convulsive seizures prompted their quantification in absolute counts per genotype.

*** The very rare EEG abnormalities observed in wild types were morphologically different from those seen in the mutants. They were represented by low to moderate voltage broad based sharp waves or low voltage sharp spikes not followed by a slow wave. Their morphological attributes were consistent with non-epileptiform sharp transients as opposed to the abnormal waveforms found in the mutant lines. There were no partial or generalized convulsive seizures observed in wild type littermates.

**** The ECG abnormalities seen most frequently in the mutant animals were premature atrial complexes, atrial fibrillation with runs of ventricular tachycardia, atrial flutter, and episodic atrio-ventricular conduction block. The sole ECG abnormality seen in both *A340E* and *T311I* wild type littermates were rare premature ventricular complexes.